Growth kinetics for a system with a conserved order parameter: Off-critical quenches

Gene F. Mazenko and Robert A. Wickham
The James Franck Institute and the Department of Physics, The University of Chicago, Chicago, Illinois 60637
(Received 24 October 1994)

The theory of growth kinetics developed previously [G. F. Mazenko, Phys. Rev. E **50**, 3485 (1994)] is extended to the asymmetric case of off-critical quenches for systems with a conserved scalar order parameter. In this instance, the new parameter M, the average global value of the order parameter, enters the theory. For $M=0$ one has critical quenches, while for sufficiently large M one approaches the coexistence curve. For all M, the theory supports a scaling solution for the order parameter correlation function with the Lifshitz-Slyozov-Wagner growth law $L\sim t^{1/3}$. The theoretically determined scaling function depends only on the spatial dimensionality d and the parameter M, and is determined explicitly here in two and three dimensions. Near the coexistence curve oscillations in the scaling function are suppressed. The structure factor displays Porod's law $Q^{-(d+1)}$ behavior at large scaled wave number Q, and Q^4 behavior at small wave number, for all M. The peak in the structure factor widens as M increases and develops a significant tail for quenches near the coexistence curve. This is in qualitative agreement with simulations.

PACS number(s): 64.60.Cn, 64.75.+g, 81.30.Hd

I. INTRODUCTION

In previous work [1], a theory based on a field-theoretic Langevin model was developed to treat the growth kinetics of a system with a conserved scalar order parameter for the case of symmetric or critical quenches. In this paper, the lowest order version of this theory is extended to off-critical quenches. Quenches to a final state near the coexistence curve where the volume fraction of the minority phase is small have been studied using a variety of approaches, but theoretical studies of the Langevin model have never been extended into this regime. The techniques developed thus far are generalizations of the Lifshitz-Slyosov-Wagner (LSW) treatment [2,3], which considers one spherical droplet interacting with a mean concentration field. This approach is valid only in the limit of zero volume fraction, but other mean field-theoretic and statistical mechanical techniques have been developed to incorporate the effects of the interaction of other droplets and extend the theory to slightly larger volume fractions [4–12]. Another approach to the problem is to use numerical simulations in concert with a theory describing the concentration field around spherical droplets (essentially an electrostatics problem with moving boundary conditions) [13]. Direct simulations of the Langevin equation exist for the off-critical case in two dimensions [14,15], but we are not aware of any such simulations for three dimensions [16].

The theory developed in [1] shows how one can solve some of the thorny problems associated with growth kinetics for the conserved order parameter (COP) case. The theory can be evaluated as a well defined sequence of approximations with qualitative and quantitative improvement as one moves along this sequence [17]. In this paper, we limit ourselves to the lowest order approximation in this formalism. From the work in [1] we know that there are substantial limitations associated with this approximation and these are discussed in some detail in Sec. VI. However, it is also known from [1] that this approximation gives good results for the scaling function for correlations of the order parameter. We therefore concentrate on this quantity here.

The new element in this work compared to [1] is that the average value of the scalar order parameter ψ is no longer zero:

$$\langle \psi(\mathbf{R},t)\rangle = M \ . \tag{1.1}$$

M is independent of $\mathbf{R}$ and t because of the statistical homogeneity of the system and the conservation law, respectively.

The main results of this paper are that, as in the critical case, the theory supports a long-time scaling solution for the order parameter correlation function,

$$C(\mathbf{R},t)=\langle \delta\psi(\mathbf{R},t)\delta\psi(\mathbf{0},t)\rangle = \psi_0^2 F\left[\frac{|\mathbf{R}|}{L(t)}\right], \tag{1.2}$$

where $\delta\psi=\psi-M$, ψ_0 is the magnitude of the ordered field in equilibrium, and $L(t)$ is the characteristic length in the theory, the average size of the domains. For later convenience, we define the normalized quantity $\tilde{M}=M/\psi_0$, which ranges between -1 and 1. When $\tilde{M}=\pm 1$ the system is at the coexistence curve. It is found that, for all $\tilde{M}$ and for long times t after the quench, the growth law $L\sim t^{1/3}$ holds. For small scaled distances x $[=|\mathbf{R}|/L(t)]$, one is able to find a scaling solution of the form

$$F(x)=1-\tilde{M}^2-e^{-y^2/2}\alpha x(1+\beta_2 x+\cdots), \tag{1.3}$$

where the parameter y is related to $\tilde{M}$ by

$$\tilde{M}=erf(y/\sqrt{2}) \ . \tag{1.4}$$

Unlike the nonconserved order parameter (NCOP) case treated earlier [18], the coefficient β_2 is not zero and must be determined, along with α, as part of a nonlinear eigenvalue problem. β_2 is found to be negative for $\tilde{M}=0$ and monotonically decreases as $\tilde{M}\to 1$. Thus, in this theory, the Tomita sum rule ($\beta_2=0$) [19] is strongly broken as one approaches the coexistence curve. This appears to be an important limitation of the current theory.

The scaling function F has been determined explicitly in two and three dimensions by solving the nonlinear eigenvalue problem mentioned above. The dependence of F on $\tilde{M}$ is weak for small $\tilde{M}$. As $\tilde{M}$ increases, the first zero of F moves to larger scaled distances and the first minimum of F becomes shallower. As $\tilde{M}$ increases further, the oscillatory behavior is suppressed and the predominant behavior is that of decay, as predicted by our large y asymptotic analysis. For large $\tilde{M}$, there are oscillations at large x whose wavelength increases as one approaches the coexistence curve. These oscillations preserve the conservation law

$$\int d^d x F(x)=0 \tag{1.5}$$

despite the existence of the strong decay.

The structure factor is the Fourier transform of the correlation function and one has

$$C(\mathbf{q},t)=\psi_0^2 L^d(t)\tilde{F}(Q)\ , \tag{1.6}$$

where $Q=qL$ is a scaled wave number. $\tilde{F}(Q)$ is characterized by five parameters. Since $\tilde{F}(Q)$ is a peaked quantity, the peak position $Q_{\max}$ and height $\tilde{F}(Q_{\max})$ are of interest as functions of $\tilde{M}$. The full width at half maximum, measured in units of $Q_{\max}$ is also relevant. The linear term in (1.3) leads to Porod's law [20] for the large Q tail of the structure factor

$$\tilde{F}(Q)=\tilde{F}(Q_{\max})A_P(\tilde{M})\left[\frac{Q}{Q_{\max}}\right]^{-(d+1)}\ , \tag{1.7}$$

while for small Q, $\tilde{F}(Q)$ behaves as [21]

$$\tilde{F}(Q)=\tilde{F}(Q_{\max})A_4(\tilde{M})\left[\frac{Q}{Q_{\max}}\right]^{4}\ . \tag{1.8}$$

This behavior at small Q is a result of a conserved diffusive field, existing away from the interfaces, which mediates the interaction among the interfaces. Our analysis shows that both $Q_{\max}$ and $\tilde{F}(Q_{\max})$ decrease to zero as $\tilde{M}\to 1$. The width of the peak increases slightly for small $\tilde{M}$, but then develops a significant tail as $\tilde{M}\to 1$ for intermediate values of Q near the base of the peak. $A_P(\tilde{M})$ is a decreasing function of $\tilde{M}$, approaching zero in a cusp as $\tilde{M}\to 1$. The coefficient $A_4(\tilde{M})$ increases with increasing $\tilde{M}$, growing rapidly near $\tilde{M}=1$. Damped oscillations are seen in the structure factor around the Q^{-4} behavior at intermediate values of Q, a result found by other investigators [22,13].

When we compare our results with those of other workers, we find good qualitative agreement for both $F(x)$ and $\tilde{F}(Q)$ as functions of $\tilde{M}$. There are some quantitative differences, though. We believe that the difference in the form of $\tilde{F}(Q)$ is due to our low estimate for the coefficient A_4, leading to a peak in $\tilde{F}(Q)$ which is too narrow. It seems likely that the lack of quantitative agreement is associated with the breaking of the Tomita sum rule in the theory. On the other hand, this is the only theory that has led to a determination of A_4, and one can hope that using higher order approximations will give improved results.

In the next section, the theory forming the basis for this work is outlined. In Sec. III the averages are performed that are relevant to the off-critical case. The end result of these manipulations is a nonlinear equation for the scaling function. Section IV looks at the various limiting cases of the theory: the small x, large x, small Q, and large y behavior. Section V presents the numerical study of the equation for $F(x)$ in two and three dimensions. Comparison of the results of this paper with results from other investigators is made in Sec. VI. The paper concludes with some comments about future areas of research and improvements to the theory.

II. THE MODEL

The dynamics are modeled using a noiseless time-dependent Ginzburg-Landau equation for a conserved scalar order parameter ψ with a nonzero average M:

$$\frac{\partial\psi(1)}{\partial t_1}=D_0\nabla_1^2[V'(\psi(1))-\nabla_1^2\psi(1)]\ . \tag{2.1}$$

$V(\psi)$ is a double-well potential with degenerate minima at $\pm\psi_0$, but is otherwise unspecified since, as we shall see, our results are independent of the precise form of V [23]. Here, the convenient notation in which 1 represents $(\mathbf{R}_1,t_1)$ is used. The $D_0\nabla_1^2$ factor in (2.1) ensures that the system has a conserved order parameter. Thermal sources of noise are neglected because it is assumed here that the quench is to zero temperature. Randomness enters the problem through the initial conditions where we assume that the initial values of $\delta\psi=\psi-M$ are governed by a Gaussian probability distribution characterized by

$$\langle\psi(\mathbf{R},0)\rangle=M\ , \tag{2.2}$$

$$\langle\delta\psi(\mathbf{R},0)\delta\psi(\mathbf{R}',0)\rangle=\epsilon_0\delta(\mathbf{R}-\mathbf{R}')\ . \tag{2.3}$$

Our final results are independent of the amplitude ϵ_0 appearing in the initial distribution.

A method of extracting the correlation functions from (2.1) is described in [1]. Here we will merely outline the salient points. The order parameter is written as

$$\psi(1)=\sigma(m(1))-u(1)\ , \tag{2.4}$$

where σ is the equilibrium interfacial profile and u represents fluctuations about this ordered value. m is assumed to be a random field whose zeros correspond to the zeros of σ, that is, to the positions of the interfaces. The nature and interpretation of m will be discussed below. In the NCOP case, the fluctuating field u can be safely ignored, but in the COP case, it is the field u which couples distant interfaces by permitting currents of minority phase atoms to flow through the matrix. In [1]

the theory was closed by relating u back to σ and m via the equation

$$u(1)=\frac{u_0}{L}\sigma(1)+\lambda\nabla_1^2 m(1)+\cdots , \tag{2.5}$$

where u_0 and λ are parameters. This form satisfies the desired properties that u is conserved in bulk, odd in m, and $O(1/L)$ everywhere. This last requirement comes from the fact that the interfaces are a source of u with a contribution proportional to the local curvature of an interface $\kappa(u|_S\sim\kappa)$. It can then be shown that if (2.5) holds, u satisfies the familiar form $\nabla^2 u=0$ away from the interfaces. σ is chosen to satisfy the equation for an equilibrium interface

$$\tfrac{1}{2}\sigma_2(1)=V'(\sigma(m(1))) , \tag{2.6}$$

where the factor $\frac{1}{2}$ is inserted for convenience and $\sigma_n(m)=\partial^n\sigma(m)/\partial m^n$. The boundary condition $\lim_{m\to\pm\infty}\sigma=\pm\psi_0$ guarantees that the system orders at the appropriate equilibrium value of the order parameter and results in the useful relation

$$\int_{-\infty}^{\infty} dx\,\sigma_1(x)=2\psi_0 . \tag{2.7}$$

As shown in [1], Eqs. (2.5) and (2.6) can be substituted into (2.1) and the result multiplied by $\sigma(2)$ and averaged to get an equation for

$$C_{\sigma\sigma}(\mathbf{R},t)=\langle\sigma(1)\sigma(2)\rangle . \tag{2.8}$$

At late times $1/L$ is expected to be small and one finds to leading order in $1/L$,

$$\frac{1}{2}\frac{\partial}{\partial t}C_{\sigma\sigma}(\mathbf{R},t)=-D_0 q_0^2\nabla^2\left[\frac{u_0}{L}C_{\sigma\sigma}(\mathbf{R},t)+\lambda\nabla^2 C_{\sigma m}(\mathbf{R},t)\right] , \tag{2.9}$$

where, $q_0^2\equiv\langle V''(\sigma)\rangle=V''(\psi_0)+O(1/L)$ and $C_{\sigma m}(\mathbf{R},t)=\langle\sigma(1)m(2)\rangle$. Here, equal times are considered and statistical homogeneity of the system has been assumed so $t_1=t_2=t$ and $\mathbf{R}=\mathbf{R}_2-\mathbf{R}_1$. Since

$$C(\mathbf{R},t)=\langle\delta\psi(1)\delta\psi(2)\rangle=\langle\sigma(1)\sigma(2)\rangle-M^2+O\left[\frac{1}{L}\right] , \tag{2.10}$$

we see that (2.9) is an equation for $C(\mathbf{R},t)$ to $O(1/L)$, since the action of the derivatives eliminates the disconnected part of the correlation function.

A key aspect of the theory is the choice of the probability distribution $P[m]$ governing the field m. This point is discussed in some detail in Refs. [1,17,24]. Here we limit ourselves to the case where $P[m]$ is given by an offset Gaussian with

$$\overline{m}(t)=\langle m(1)\rangle_0 , \tag{2.11}$$

and $\langle\ \rangle_0$ is over a probability distribution $P_0[\delta m]$ which is Gaussian with respect to $\delta m(1)=m(1)-\overline{m}(t)$. $P_0[\delta m]$ is then determined by the variance

$$C_0(12)=\langle\delta m(1)\delta m(2)\rangle_0 . \tag{2.12}$$

Since the field m can be approximately interpreted as the perpendicular distance to the nearest interface, the offset corresponds to a greater probability of being in one phase than in the other. The effects of this nonzero average will be explored in the next section.

III. EVALUATION OF AVERAGES: THE SCALING EQUATION OF MOTION

A. Evaluation of averages

In order for (2.9) to be a closed equation for $C_{\sigma\sigma}$, it is necessary to relate $C_{\sigma m}$ to $C_{\sigma\sigma}$. As in [1], this is done by using the Gaussian nature of m. Now, however, the Gaussian probability distribution must satisfy the condition $\langle m(1)\rangle_0=\overline{m}(t)\neq 0$. Taking this into account, one finds, using the standard properties of Gaussian integrals [18],

$$C_{\sigma m}(12)=\langle\sigma_1(1)\rangle_0 C_0(12)+M\overline{m}(t) . \tag{3.1}$$

The spatially independent term is eliminated by the action of the Laplacian in (2.9). Since m is a Gaussian random field, it follows that

$$\langle\sigma_1(1)\rangle_0=\int dx_1\sigma_1(x_1)\Phi(x_1) , \tag{3.2}$$

where

$$\Phi(x_1)=\frac{1}{\sqrt{2\pi S_0(t)}}e^{-(1/2)[x_1-\overline{m}(t)]^2/S_0(t)} , \tag{3.3}$$

with

$$S_0(t)=C_0(11) . \tag{3.4}$$

Since m is a measure of the distance away from an interface, it is expected that in the long-time scaling regime $S_0\sim L^2$ and $\overline{m}(t)\sim L$. Therefore, the limit

$$\lim_{t\to\infty}\frac{\overline{m}(t)}{\sqrt{S_0(t)}}=y \tag{3.5}$$

exists. In evaluating (3.2), it is important to note that for a wide class of potentials, $\sigma_1(x_1)$ goes exponentially to zero for large $|x_1|$. Therefore, one can, after eliminating $\overline{m}$ in favor of $y\sqrt{S_0(t)}$, expand (3.2) in powers of S_0^{-1} and use (2.7) to obtain

$$\langle\sigma_1(1)\rangle_0=\frac{2\psi_0}{\sqrt{2\pi S_0(t)}}e^{-(1/2)y^2}+O(S_0^{-1}) . \tag{3.6}$$

The parameter y can be related to M by using the derivative relation [25]

$$\frac{\partial M}{\partial\overline{m}(t)}=\frac{\partial\langle\sigma\rangle_0}{\partial\overline{m}(t)}=\langle\sigma_1\rangle_0 , \tag{3.7}$$

from which follows

$$M=\int_0^{\overline{m}(t)}dz\left[\frac{2}{\pi S_0(t)}\right]^{1/2}\psi_0 e^{-\frac{1}{2}[z^2/S_0(t)]} . \tag{3.8}$$

Thus, with $\tilde{M}=M/\psi_0$,

$$\tilde{M}=\mathrm{erf}(y/\sqrt{2}) \ . \tag{3.9}$$

Therefore, there is a one-to-one correspondence between y and $\tilde{M}$. $y=0$ is a critical quench and $y\to\infty$ corresponds to a quench at the coexistence curve.

With the definition

$$f(\mathbf{R},t)=\frac{C_0(\mathbf{R},t)}{S_0(t)} \tag{3.10}$$

and the use of (3.1) and (3.6), the equation of motion (2.9) takes the form

$$\frac{1}{2}\frac{\partial}{\partial t}C_{\sigma\sigma}(\mathbf{R},t)=-D_0q_0^2\nabla^2\left[\frac{u_0}{L}C_{\sigma\sigma}(\mathbf{R},t)+\lambda\left[\frac{2S_0}{\pi}\right]^{1/2}\psi_0 e^{-\frac{1}{2}y^2}\nabla^2 f(\mathbf{R},t)\right] . \tag{3.11}$$

The theory can be closed by relating $C_0(\mathbf{R},t)$ to $C_{\sigma\sigma}(\mathbf{R},t)$ via the relation [18]

$$C_{11}(\mathbf{R},t)=\frac{\partial C_{\sigma\sigma}(\mathbf{R},t)}{\partial C_0(\mathbf{R},t)} , \tag{3.12}$$

where $C_{nm}(\mathbf{R},t)=\langle\sigma_n(1)\sigma_m(2)\rangle_0$. The fact that m is Gaussian enables one to write

$$C_{11}(\mathbf{R},t)=\int dx_1dx_2\sigma_1(x_1)\sigma_1(x_2)\Phi(x_1,x_2) , \tag{3.13}$$

where

$$\Phi(x_1,x_2)=\frac{\gamma}{2\pi S_0}e^{-(1/2)(\gamma^2/S_0)\{[x_1-\bar{m}(t)]^2+[x_2-\bar{m}(t)]^2-2f[x_1-\bar{m}(t)][x_2-\bar{m}(t)]\}} , \tag{3.14}$$

with $\gamma=(1-f^2)^{-\frac{1}{2}}$. Again, $\bar{m}(t)$ can be eliminated in favor of $y\sqrt{S_0(t)}$ and the result (3.13) expanded in terms of S_0^{-1}. At long times, the leading order term dominates, resulting in

$$C_{11}(\mathbf{R},t)=\frac{\gamma}{2\pi S_0}e^{-y^2/(1+f)}\int dx_1dx_2\sigma_1(x_1)\sigma_1(x_2)+O(S_0^{-3/2}) , \tag{3.15}$$

where the integral is easily found to give $4\psi_0^2$. Integration of (3.12) with the substitution (3.15), keeping in mind the definition of f, gives the desired relation between $C_{\sigma\sigma}$ and f,

$$C_{\sigma\sigma}=\frac{2\psi_0^2}{\pi}\int_0^f\frac{ds}{\sqrt{1-s^2}}e^{-y^2/(1+s)} . \tag{3.16}$$

For a critical quench $y=0$, and this reduces to the now standard expression $C_{\sigma\sigma}=(2/\pi)\psi_0^2\sin^{-1}f$. Equations (3.16) and (3.11) form a closed system of equations for $C_{\sigma\sigma}$.

B. The scaling regime

At long times, the correlation function is expected to have a scaling solution. The ansatz

$$C_{\sigma\sigma}(\mathbf{R},t)=\psi_0^2F(x) , \tag{3.17}$$

with $x=|\mathbf{R}|/L(t)$ being the scaled distance, can be substituted into Eqs. (3.11) and (3.16) to give

$$x\bar{F}'=\nabla^2(\bar{u}\bar{F}+\nabla^2 f), \tag{3.18}$$

$$\bar{F}=\frac{2}{\pi}\int_0^f\frac{ds}{\sqrt{1-s^2}}e^{-(1/2)y^2(1-s)/(1+s)} , \tag{3.19}$$

where

$$\bar{F}(x)=e^{y^2/2}F(x) , \tag{3.20}$$

$$\bar{u}=\frac{2u_0D_0q_0^2}{L^2\dot{L}} , \tag{3.21}$$

and we have chosen $L=(\lambda\bar{u}/\psi_0u_0)\sqrt{2S_0/\pi}$. Note that for scaling we require that $\bar{u}$ be a constant and therefore $L\sim t^{1/3}$. One expects $\bar{F}$ to have a weaker y dependence than F for large y. It is useful to express f in terms of

$$\Phi=\left[\frac{1-f}{1+f}\right]^{1/2} \tag{3.22}$$

in Eq. (3.19) to obtain the well behaved integral representation

$$\bar{F}=\frac{4}{\pi}\int_\Phi^1\frac{ds}{1+s^2}e^{(-y^2s^2)/2} . \tag{3.23}$$

For future reference, the spatial derivative of (3.23) is

$$\frac{\partial\bar{F}}{\partial x}=-\frac{4}{\pi}\frac{e^{(-y^2\Phi^2)/2}}{1+\Phi^2}\frac{\partial\Phi}{\partial x} . \tag{3.24}$$

It is noteworthy that $\bar{F}$ has a lower bound. Let $\Phi\to\infty$ in (3.23) and write

$$\bar{F}_{\min}=\frac{4}{\pi}e^{y^2/2}\int_\infty^1\frac{ds}{1+s^2}e^{-(y^2/2)(1+s^2)}=\frac{4}{\pi}e^{y^2/2}I(y) . \tag{3.25}$$

$I(y)$ has the following properties:

$$I(0)=-\frac{\pi}{4} ,$$

$$\frac{d}{dy}I(y)=\frac{\pi}{2}\left[1-erf\left[\frac{y}{\sqrt{2}}\right]\right]\frac{d}{dy}erf\left[\frac{y}{\sqrt{2}}\right] . \quad (3.26)$$

Integrating these equations yields

$$I(y)=-\frac{\pi}{4}\left[1-erf\left[\frac{y}{\sqrt{2}}\right]\right]^2=-\frac{\pi}{4}(1-|\tilde{M}|)^2 . \quad (3.27)$$

Thus, the lower bound on $\bar{F}$ is

$$\bar{F}_{\min}=-e^{y^2/2}(1-|\tilde{M}|)^2 . \quad (3.28)$$

As $\tilde{M}\to 1$ this lower bound approaches zero.

Equations (3.18) and (3.23) constitute a nonlinear eigenvalue problem for $\bar{F}$, with a unique solution determined by the boundary conditions at small x and the physical condition $\bar{F}\to 0$ exponentially as $x\to\infty$. We will see that $\bar{u}$ is determined as part of the solution. The only parameters entering into the determination of $\bar{F}$ are y and the dimension d, which appears in the spherically symmetric Laplacian.

IV. LIMITING CASES

A. Small x behavior

The small x behavior of $\bar{F}$ can be determined analytically. We find that $\bar{F}$ has the form

$$\bar{F}=\bar{F}(0)-\alpha x(1+\beta_2 x^2+\beta_3 x^3+\cdots) . \quad (4.1)$$

Expanding Φ for small x,

$$\Phi=\Phi_1 x+\Phi_2 x^2+\cdots \quad (4.2)$$

and using (3.24) to connect the power series for $\bar{F}$ and Φ gives

$$\Phi_1=\frac{\pi\alpha}{4} , \quad (4.3)$$

$$\Phi_2=\frac{\pi\alpha\beta_2}{4} . \quad (4.4)$$

Substitution of these results into (3.18) gives, at $O(1/x)$,

$$\bar{u}=\frac{-3\pi^2\alpha\beta_2(d+1)}{4} . \quad (4.5)$$

$\bar{F}(0)$ can be determined from (3.23) by noting that $\Phi(0)=0$ and then using the same technique that was used to derive (3.28). The result is

$$\bar{F}(0)=(1-\tilde{M}^2)e^{y^2/2} . \quad (4.6)$$

The equation of motion (3.18) can be partially integrated using the Green's function for the Laplacian [25]. For $d>2$, the result is

$$\bar{u}\bar{F}+\nabla^2 f=\frac{1}{d-2}\left[\frac{d}{x^{d-2}}I_d(x)-2[I_2(x)-I_2(\infty)]\right] , \quad (4.7)$$

with

$$I_d(x)=\int_0^x z^{d-1}\bar{F}(z)dz . \quad (4.8)$$

The results (4.3) and (4.4) can be substituted into (4.7). Since one can show that

$$\lim_{x\to 0}\frac{I_d(x)}{x^{d-2}}=\lim_{x\to 0}I_2(x)=0 , \quad (4.9)$$

one has at $O(1)$

$$\frac{2}{d-2}I_2(\infty)=-\frac{\pi^2\alpha^2 d}{4}+\bar{u}\bar{F}(0) . \quad (4.10)$$

For $d=2$, the analogous results are

$$\bar{u}\bar{F}+\nabla^2 f=(1-2\ln x)I_2(x)+2[J_2(x)-J_2(\infty)] , \quad (4.11)$$

with

$$J_2(x)=\int_0^x dz\, z\bar{F}(z)\ln z . \quad (4.12)$$

Since $\lim_{x\to 0}J_2(x)=0$, substitution of (4.3) and (4.4) into (4.11) gives, at $O(1)$,

$$-2J_2(\infty)=-\frac{\pi^2\alpha^2}{2}+\bar{u}\bar{F}(0) . \quad (4.13)$$

Knowledge of the parameters α and β_2 allows one to determine the constants $\bar{u}$ and $I_2(\infty)$ [or $J_2(\infty)$] appearing in the equation of motion for a given value of y. Numerically, what this means is that values for α and β_2 are chosen and Eqs. (4.7) [or (4.11)] and (3.23) integrated forward in x. α and β_2 are adjusted until $\bar{F}$ satisfies both the conservation law (1.5) and the boundary condition $\bar{F}\to 0$ exponentially as $x\to\infty$.

B. Large x behavior

For large x, both $\bar{F}$ and f are small and Φ can be expanded about its asymptotic value

$$\Phi(x)=1+\eta(x) . \quad (4.14)$$

Substitution into (3.24) and integration yields a relation between $\bar{F}$ and η:

$$\bar{F}(x)=-\frac{2}{\pi}e^{-y^2/2}\eta(x) . \quad (4.15)$$

Also, from (3.22) we have $f(x)=-\eta(x)$, so we may write (3.18) in the large-x limit as

$$x\bar{F}'=\nabla^2(\bar{u}\bar{F}+\frac{\pi}{2}e^{y^2/2}\nabla^2\bar{F}) . \quad (4.16)$$

This equation supports damped oscillatory solutions of the form

$$\bar{F}\sim\bar{F}_0 x^{-2d/3}\exp\left[-\frac{3e^{-y^2/6}}{2^{8/3}\pi^{1/3}}x^{4/3}\right]$$

$$\times\cos\left[\frac{3^{3/2}e^{-y^2/6}}{2^{8/3}\pi^{1/3}}x^{4/3}+\phi\right] , \quad (4.17)$$

where $\bar{F}_0$ and ϕ are constants. Note that as $y\to\infty$ the wavelength of the oscillations increases and the exponential term goes to 1. This means that in this limit one

must go to progressively larger values of x before one sees this asymptotic behavior.

C. Small Q behavior

It is the Fourier transform of the order parameter correlation function,

$$C(\mathbf{q},t)=\int d^d\mathbf{R}e^{i\mathbf{q}\cdot\mathbf{R}}\langle\psi(\mathbf{R},t)\psi(\mathbf{0},t)\rangle$$
$$=\psi_0^2L^d(t)\tilde{F}(Q)+(2\pi)^dM^2\delta(q)\ , \tag{4.18}$$

with $Q=qL(t)$, and it is

$$\tilde{F}(Q)=\int d^dx e^{i\mathbf{Q}\cdot\mathbf{x}}F(x)\ , \tag{4.19}$$

that is measured in a scattering experiment. In the total scattering cross section, we expect that at long times there is a dynamic contribution to the forward Bragg peak,

$$\lim_{t\to\infty}\psi_0^2L^d(t)\tilde{F}(Q)=A\,\delta(q)\ , \tag{4.20}$$

in addition to the static contribution $(2\pi)^dM^2\delta(q)$. Since

$$A=\int d^dq\lim_{t\to\infty}\psi_0^2L^d(t)\tilde{F}(Q)$$
$$=(2\pi)^d\psi_0^2F(0)=(2\pi)^d\psi_0^2(1-\bar{M}^2)\ , \tag{4.21}$$

the total contribution to the forward Bragg peak at late times is $(2\pi)^d\psi_0^2\delta(q)$, as expected.

To examine the small Q behavior of the structure factor $\tilde{F}(Q)$, it is useful to consider the moments of $F(x)$

$$W_p=\int d^dx x^pF(x)\ , \tag{4.22}$$

which can be found by multiplying (3.18) by x^p and integrating. The result is that $W_0=W_2=0$, while

$$W_4=-\frac{8d(d+2)}{d+4}e^{-(1/2)y^2}\int d^dx f(x)\ . \tag{4.23}$$

Thus we have

$$\tilde{F}(Q)\sim AQ^4 \tag{4.24}$$

for small Q, where

$$A=-\frac{e^{-y^2/2}}{d+4}\int d^dx f(x)\ . \tag{4.25}$$

The Q^4 behavior of $\tilde{F}(Q)$ at small Q is a consequence of the fact that in the theory, u is conserved away from the interfaces, and this behavior does not depend on the specific ansatz for u. Later, when we integrate the equation of motion (4.7) [or (4.11)], we find that $\tilde{F}(Q)$ is positive definite and that

$$\int d^dx f(x)<0\ , \tag{4.26}$$

consistent with Eqs. (4.24) and (4.25). Although the physical observable $\tilde{F}(Q)$ is positive, there exists a mathematical difficulty because Eq. (4.26) implies that $\lim_{q\to0}\langle|m_q(t)|^2\rangle/S_0<0$. As pointed out by Yeung, Oono, and Shinozaki [26], this is a shortcoming of the fact that the auxiliary field m is a Gaussian variable. This problem can be resolved by considering non-Gaussian corrections to the probability distribution for the field m [1].

D. Large y behavior

An analytic result for the limit as one approaches the coexistence curve, $\bar{M}\to1$, $y\to\infty$, is of interest because it allows one to make comparisons with other theories developed for this regime. From the numerical analysis in the next section, the following facts emerge. The first is that as y increases, the scaled length x over which the correlation function takes significant values decreases. This suggests that x should be rescaled as

$$x=y^pz \tag{4.27}$$

with $p<0$. Second, it appears that $\bar{u}$ grows as some power of y for large y. We are led to assume the form

$$\bar{u}=\bar{u}_\infty y^n\ , \tag{4.28}$$

with $n>1$. Finally, since the interesting behavior occurs near the origin where the quantity Φ is small, we can rescale Φ

$$\Phi=\frac{\phi}{y}\ll1\ , \tag{4.29}$$

where ϕ grows slowly but does not break the bound near the origin. Using this definition in Eq. (3.22) leads to

$$f\approx1-2\frac{\phi^2}{y^2}\ . \tag{4.30}$$

Armed with these results, we proceed to re-examine the theory. Using (4.29) in Eq. (3.23) and letting $t=ys$ in the integrand gives

$$\bar{F}(z)=\frac{4}{\pi y}\int_{\phi(z)}^{y}\frac{dt}{1+(t/y)^2}e^{-t^2/2}\ . \tag{4.31}$$

To leading order in y^{-1} this is

$$\bar{F}(z)=\frac{4}{\pi y}\int_{\phi(z)}^{\infty}dt\,e^{-t^2/2}=\frac{1}{y}\bar{F}_\infty(z)\ , \tag{4.32}$$

where

$$\bar{F}_\infty(z)=2\left[\frac{2}{\pi}\right]^{1/2}\left[1-erf\left[\frac{\phi(z)}{\sqrt{2}}\right]\right]\ . \tag{4.33}$$

Under the rescaling outlined above, the equation of motion (4.7) for $d>2$ becomes

$$\bar{u}_\infty y^{n-1}\bar{F}_\infty(z)-2y^{-2(p+1)}\nabla_z^2\phi^2$$
$$=\frac{y^{2p-1}}{d-2}\left[\frac{d}{z^{d-2}}I_d(z)-2[I_2(z)-I_2(\infty)]\right]\ , \tag{4.34}$$

with

$$I_d(z)=\int_0^z ds\,s^{d-1}\bar{F}_\infty(s)\ . \tag{4.35}$$

Since $p<0$, the right hand side does not contribute as $y\to\infty$. The integrals in the $d=2$ case also do not contribute in this limit, so the following results are valid for $d\geq2$. Balancing powers of y on the left hand side of (4.34) gives

$$p=-\frac{n+1}{2} \tag{4.36}$$

and

$$\bar{u}_\infty \bar{F}_\infty(z)-2\nabla^2\phi^2=0 \ . \tag{4.37}$$

Using (4.33), this becomes a simple equation for ϕ

$$\bar{u}_\infty \left[\frac{2}{\pi}\right]^{1/2}\left[1-erf\left[\frac{\phi}{\sqrt{2}}\right]\right]=\nabla^2\phi^2 \ . \tag{4.38}$$

In the numerical solution of (4.38), $\bar{u}_\infty$ is a parameter found from a fit of the numerically determined $\bar{u}$ to the form (4.28) for large y.

E. Small and large z behavior for large y

An examination of (4.38) in the limit of large and small z is instructive. When z is small, ϕ is expected to be small so ϕ can be expanded as a power series in z,

$$\phi=\phi_1 z+\phi_2 z^2+\cdots \ . \tag{4.39}$$

Also, in this limit, (4.38) simplifies to the form

$$\bar{u}_\infty \left[\frac{2}{\pi}\right]^{1/2}\left[1-\left[\frac{2}{\pi}\right]^{1/2}\phi\right]=\nabla^2\phi^2 \ . \tag{4.40}$$

Matching powers of z to leading order gives

$$\phi_1=\left[\frac{2}{\pi}\right]^{1/4}\left[\frac{\bar{u}_\infty}{2d}\right]^{1/2} \ . \tag{4.41}$$

This result allows one to make predictions about the asymptotic behavior of α and β_2 when y is large. Using (4.27) and (4.33), one can write

$$\bar{F}(x)=\frac{2}{y}\left[\frac{2}{\pi}\right]^{1/2}-\frac{4}{\pi}\phi_1 y^{-p-1}x+\cdots \ , \tag{4.42}$$

giving

$$\alpha=\alpha_\infty y^{-p-1} \tag{4.43}$$

for large y with $\alpha_\infty=4\phi_1/\pi$. If we also write

$$\beta_2=\beta_{2\infty}y^m \ , \tag{4.44}$$

then

$$\bar{u}=-\frac{3\pi^2\alpha_\infty\beta_{2\infty}(d+1)}{4}y^{m-p-1}=\bar{u}_\infty y^n \ . \tag{4.45}$$

Matching the coefficient and the exponent leads, using (4.36), to the following relationships:

$$\alpha=\alpha_\infty y^{(n-1)/2} \ , \tag{4.46}$$

$$\beta_2=\beta_{2\infty}y^{(n+1)/2} \ , \tag{4.47}$$

$$\alpha_\infty=-\frac{12}{\sqrt{2\pi}}\left[\frac{d+1}{d}\right]\beta_{2\infty} \ . \tag{4.48}$$

Thus, a graph of β_2/α vs y for large y will be linear with a slope that depends only on the dimensionality of the system.

At large z, ϕ is large and (4.38) is well approximated by

$$\bar{u}_\infty\frac{2}{\pi\phi}e^{-\phi^2/2}=\nabla^2\phi^2 \ . \tag{4.49}$$

For $d>2$, standard asymptotic analysis yields, at next to leading order,

$$\phi(z)=\ln^{1/2}\left[\frac{z^4}{\ln z}\left[\frac{\bar{u}_\infty}{2\pi(d-2)}\right]^2\right] \ . \tag{4.50}$$

This implies that

$$\bar{F}_\infty(z)=\frac{4(d-2)}{\bar{u}_\infty}\frac{1}{z^2} \tag{4.51}$$

for large z and $d>2$. For $d=2$ one has

$$\bar{F}_\infty(z)=\frac{\bar{F}_0}{(1+(\bar{u}_\infty\bar{F}_0)/16z^2)^2} \ . \tag{4.52}$$

It is clear that near the coexistence curve, the oscillations in the scaling form become insignificant and are dominated by a strong decay.

V. NUMERICAL SOLUTION OF THE NONLINEAR EIGENVALUE PROBLEM

A. α and β_2 as a function of y

In this section, the numerical solution of (4.7) [or (4.11)] coupled with (3.23) in two and three dimensions will be discussed. The equations are integrated forward from $x=0$ using a fourth order Runge-Kutta integrator with step size $\delta x=0.001$, subject to the initial conditions $\bar{F}(0)=(1-\tilde{M}^2)e^{y^2/2}$, $\bar{F}'(0)=-\alpha$, $\bar{F}''(0)=-2\alpha\beta_2$, and $f'(0)=0$. This method of integration seems numerically stable and insensitive to the choice of δx. The search for the eigenvalues α and β_2 involves requiring that the solution $\bar{F}$ obey the conservation law (1.5) and have the physically acceptable behavior $\bar{F}\to 0$ exponentially as $x\to\infty$. This search is performed by fixing α and then searching for the value of β_2 that pushes the diverging, unphysical solution to larger values of x. The value of α is then adjusted so that the flat region of $\bar{F}$ at large x is properly zeroed. The procedure is repeated with the new value of α until the exponentially growing solution is pushed as far from the origin as possible and until $\bar{F}$ is zeroed as well as possible. The degree to which the conservation law is satisfied naturally depends on how well the function is zeroed. The convergence of the eigenvalues is fast and $\bar{F}$ can be zeroed to better than 10^{-6} using this method.

The results for the eigenvalues α and β_2 are shown in Fig. 1. One sees that α initially decreases, reaching a minimum at $y\sim 1$, and then rapidly becomes large and positive as the coexistence curve is approached. The eigenvalue β_2 is negative at $y=0$ and monotonically decreases as y increases, decreasing rapidly as y becomes large ($\tilde{M}\to 1$). Equation (4.48) predicts that a graph of β_2/α will be linear for large y with a slope -0.157 for $d=3$ and -0.139 for $d=2$. We see this linear behavior and have measured slopes of about -0.143 and -0.129

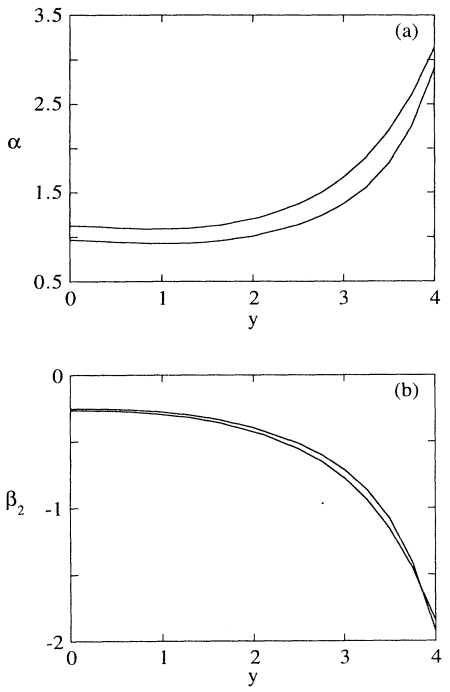

FIG. 1. The eigenvalues α and β_2 as a function of y. (a) α for two dimensions (upper curve) and three dimensions (lower curve). (b) β_2 for two dimensions (lower curve at $y=0$) and three dimensions (upper curve at $y=0$).

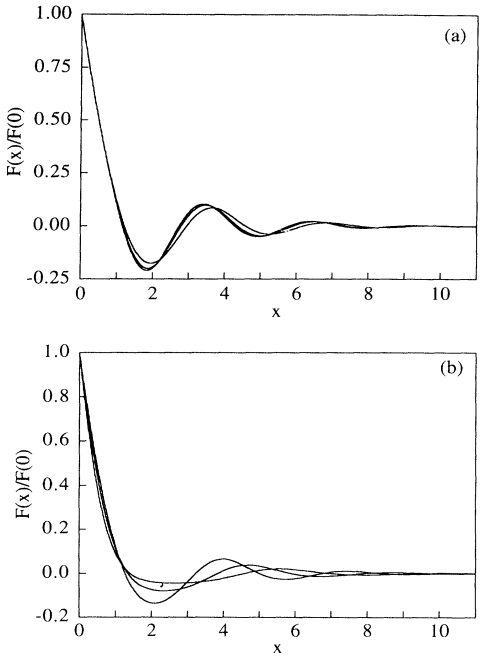

FIG. 2. The normalized scaling function $F(x)$ in two dimensions for various $\tilde{M}$. In terms of decreasing depth of the first minimum, the curves correspond to (a) $\tilde{M}=0$, 0.2, and 0.4; (b) $\tilde{M}=0.6$, 0.8, and 0.9.

for $d=2$ and 3, respectively. The exponents n and p, and the coefficient $\bar{u}_\infty$ defined in (4.27) and (4.28), can be found by fitting the large y behavior of α and β_2 to the forms (4.46) and (4.47). For three dimensions, one finds $n\sim 8$, $p\sim -4.5$, and $\bar{u}_\infty \sim 0.0033$. In two dimensions, one has $n\sim 6$, $p\sim -3.5$, and $\bar{u}_\infty \sim 0.024$. When considering these results, it should be kept in mind that only a few values of y around $y=4$ were used to obtain these values. In principle, both the exponents and the coefficient can be accurately obtained by extending the numerical analysis to larger values of y. In practice, this is difficult for reasons that are discussed below.

B. Scaling function as a function of $\tilde{M}$

The dependence of the scaling function $F(x)$ on $\tilde{M}$ is shown in Fig. 2 for two dimensions and in Fig. 3 for three dimensions. In these plots $F(x)$ is normalized so that $F(0)=1$. Both figures show that $F(x)$ depends only weakly on $\tilde{M}$ for values of $\tilde{M}<0.4$. The scaling function has a prominent oscillatory component which is necessary to satisfy the conservation law. At intermediate values of $\tilde{M}$, the position of the first minimum of $F(x)$ occurs at larger values of x and the depth of this minimum decreases as $\tilde{M}$ increases. The depth of the oscillations is greater in two dimensions than in three. These stronger oscillations make the presence of the lower bound on $F(x)$ noticeable, and near the coexistence curve the minima in the scaling function are very flat in order to be consistent with this bound.

As $\tilde{M}\to 1$ the scaling function approaches its asymp-

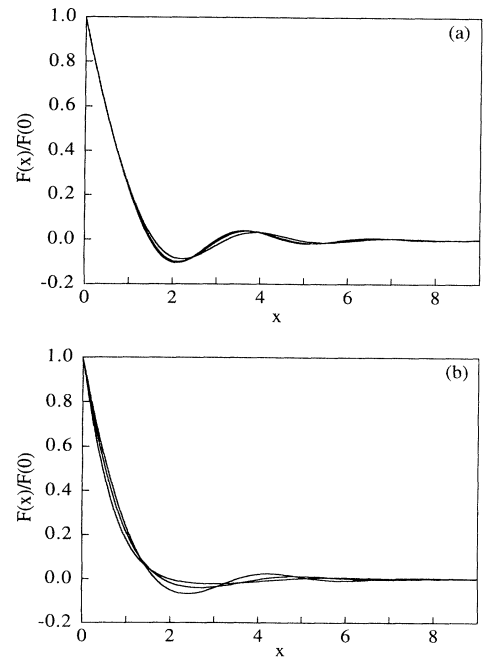

FIG. 3. The normalized scaling function $F(x)$ in three dimensions for various $\tilde{M}$. In terms of decreasing depth of the first minimum, the curves correspond to (a) $\tilde{M}=0$, 0.2, and 0.4; (b) $\tilde{M}=0.6$, 0.8, and 0.9.

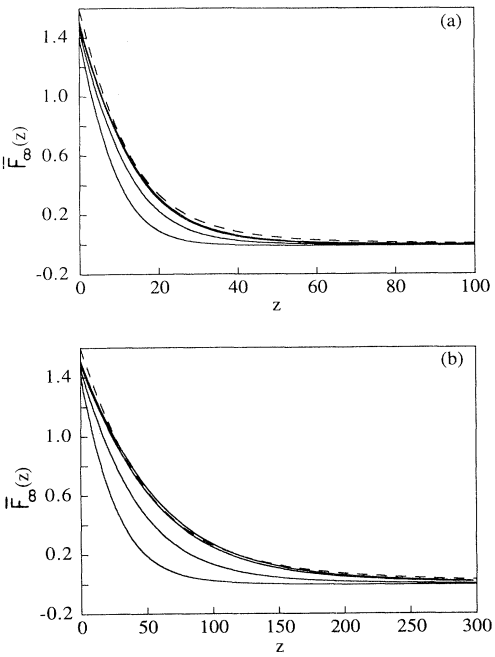

FIG. 4. The large y asymptotic scaling function $\bar{F}_\infty(z)$. From lowest to uppermost, the solid curves correspond to $y=2.5$, 3, 3.5, and 4 ($\tilde{M}=0.9876$, 0.9973, 0.9995, and 0.9999, respectively). The infinite y form ($\tilde{M}=1$), obtained from our asymptotic analysis is shown as a dashed line. (a) Two dimensions. (b) Three dimensions.

totic form (4.33) which can be determined by numerically solving (4.38) using the values of $\bar{u}_\infty$ found in the preceding section. Since we know the exponent p, we can rescale the distance x using (4.27) and plot $\bar{F}_\infty(z)=y\bar{F}(xy^{-p})$ for large values of y. This is done for two and three dimensions in Fig. 4. The asymptotic forms obtained by solving (4.38) are also shown in this figure. We see that $F(x)$ decays very rapidly when the system is near the coexistence curve. Oscillations do occur for these values of y, but they occur at large x and have a small amplitude and large wavelength. For $d=3$, the curves appear to approach the asymptotic form as y increases. However, for $d=2$ the asymptotic form is not approached if one uses $\bar{u}_\infty=0.024$. A value of $\bar{u}_\infty=0.036$ gives a better fit and the form obtained using this value is the one shown in Fig. 4. Matching the asymptotic form to the rescaled large y scaling function is another way to determine $\bar{u}_\infty$. We believe that the two methods of finding $\bar{u}_\infty$ give different values because in the fit of α and β_2 to the forms (4.46) and (4.47) we do not have values of y large enough to be in the asymptotic regime. Larger values of y are difficult to reach because one runs into numerical problems as the theoretical lower bound on $F(x)$ approaches zero. These numerical problems are especially significant in two dimensions, since the oscillations in the correlation function are stronger than in three dimensions.

C. Scaling of the structure factor

The structure factor

$$\tilde{F}(Q)=\int d^dx e^{iQ\cdot x}F(x) \tag{5.1}$$

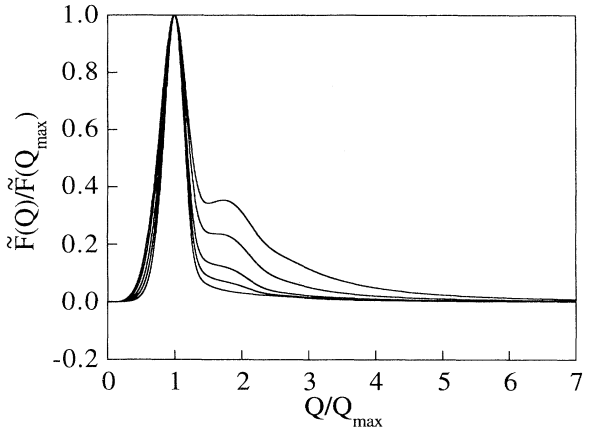

FIG. 5. The normalized structure factor in two dimensions. From lowest to uppermost, the curves correspond to $\tilde{M}=0$, 0.4, 0.6, 0.8, and 0.9.

was calculated by taking the Fourier transform of our numerically determined $F(x)$. We find that as $\tilde{M}$ increases the height of the peak decreases and the peak position moves to smaller values of Q. Graphs of the normalized structure factor for various $\tilde{M}$ are shown in Fig. 5 for $d=2$ and Fig. 6 for $d=3$. Logarithmic plots reveal the power-law dependence of $\tilde{F}(Q)$ for large and small Q (Fig. 7). For small Q, $\tilde{F}(Q)\sim Q^4$ in both $d=2$ and 3, for all $\tilde{M}$. Small deviations from the Q^4 behavior can be seen, but we attribute these to the unreliability of the numerical determination of $F(x)$ for extremely large x. For large Q, one observes Porod's law, $\tilde{F}(Q)\sim Q^{-(d+1)}$, for all $\tilde{M}$. The coefficients A_4 and A_P defined in the Introduction are determined and plotted in Figs. 8 and 9, respectively, as functions of $\tilde{M}$. A_4 increases with increasing $\tilde{M}$ and A_P is a decreasing function of $\tilde{M}$, approaching zero like a cusp at the coexistence curve.

Figures 5 and 6 show that the width of the peak increases slightly, but is rather insensitive to changes in $\tilde{M}$ until very near the coexistence curve. In the logarithmic plots there appear to be damped oscillations in $\tilde{F}(Q)$ at

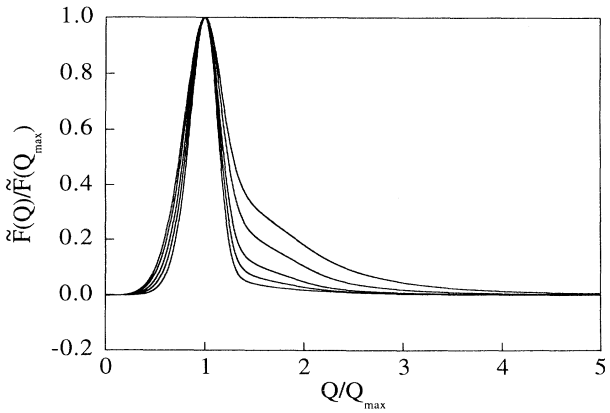

FIG. 6. The normalized structure factor in three dimensions. From lowest to uppermost, the curves correspond to $\tilde{M}=0$, 0.4, 0.6, 0.8, and 0.9.

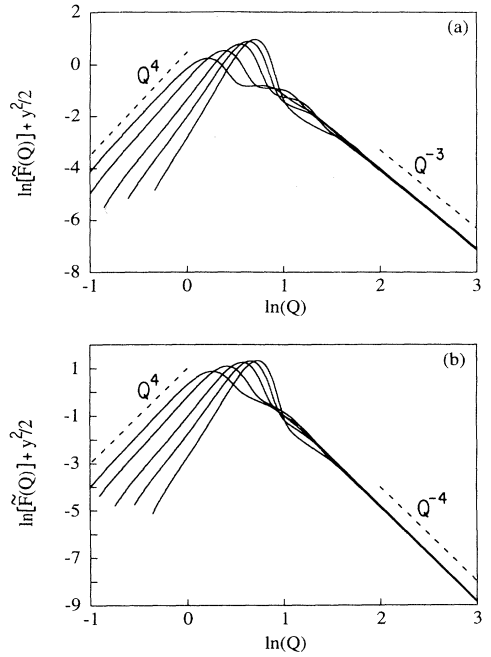

FIG. 7. Logarithmic plots of $e^{y^2/2}\tilde{F}(Q)$. At $\ln(Q)=0$, from lowest to uppermost, the curves correspond to $\tilde{M}=0$, 0.4, 0.6, 0.8, and 0.9. (a) Two dimensions. (b) Three dimensions. In both graphs, Q^4 behavior is seen at small Q and Porod's law $Q^{-(d+1)}$ behavior occurs at large Q (dotted lines).

intermediate Q before the onset of the $Q^{-(d+1)}$ behavior. In two dimensions, as one approaches the coexistence curve, the main peak decreases in amplitude until it is comparable to these oscillations, which show up as a shoulder to the main peak. In three dimensions, there is a tail on the large Q side of the peak in the structure factor, which grows as $\tilde{M}$ increases. Both the secondary peak and the tail may be related to the fact that the Tomita sum rule is strongly broken as $\tilde{M}\to 1$. The large coefficient of x^2 in the small x expansion of $\tilde{F}(x)$ will lead to corrections to Porod's law for the medium Q behavior of the structure factor.

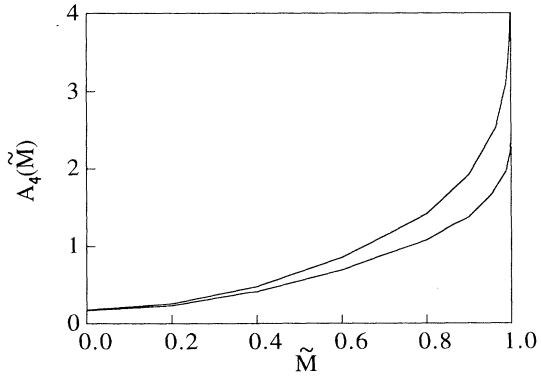

FIG. 8. The coefficient $A_4(\tilde{M})$ appearing in the small Q behavior of $\tilde{F}(Q)$ for two (upper curve) and three (lower curve) dimensions.

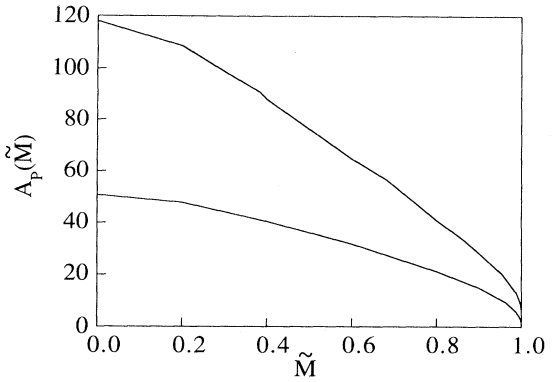

FIG. 9. The Porod's law coefficient $A_P(\tilde{M})$ for two (lower curve) and three (upper curve) dimensions.

VI. COMPARISONS

In order to test the validity of the assumptions made in this paper, the results for $F(x)$ and $\tilde{F}(Q)$ will be compared with the relevant results of other investigators. Experiments involving neutron scattering off of a binary alloy have been done for a fixed $\tilde{M}$ [27], but we have been unable to find any experimental study of the dependence of $\tilde{F}(Q)$ on $\tilde{M}$. One problem with doing experiments near the coexistence curve is that the small volume fraction of the minority phase causes the structure factor to have a small amplitude, thus making it difficult to measure. Another problem that arises when comparing experiment to theory is that it is unclear what volume fraction was used in a given experiment, making a straightforward comparison difficult.

While there are high quality numerical simulations for critical quenches [28–30], there has been far less work on off-critical quenches. One example is the direct numerical simulation of the Cahn-Hilliard equation in two dimensions performed by Chakrabarti, Toral, and Gunton [15]. Here, we compare their result for the correlation function with ours. Their functions are scaled so that the first zero of the correlation function occurs at $x=1$, and we have adjusted our length scale to correspond to this. The comparisons for volume fractions $\phi=0.5$, 0.21, and 0.05 are shown in Fig. 10. The relationship between $\tilde{M}$ and the volume fraction ϕ is

$$\phi=\tfrac{1}{2}(1-\tilde{M})\ , \tag{6.1}$$

which is valid for quenches to $T=0$. The quantitative agreement is poor. In particular, the theory predicts that at large x the oscillations in $F(x)$ have much larger amplitude than is seen in the simulations. Nevertheless, the positions of peaks and troughs of the oscillations are in qualitative agreement. In addition, we agree on the observation that oscillations in the correlation function become weaker and have longer wavelengths as the coexistence curve is approached. In summary, the qualitative agreement is reasonable. We are unaware of any direct simulation of the Cahn-Hilliard equation in three dimen-

sions for the off-critical case. Such simulations are difficult because large system sizes are required to give a statistically meaningful distribution of droplets when the volume fraction is small.

One can also make comparisons with generalizations of the LSW theory [4–12]. This is in the regime of Ostwald ripening [31]. While much of the analysis in this case has focused on the droplet distribution function, more recently a number of authors have determined $\tilde{F}(Q)$. In particular, here we will compare our three dimensional results with those of Akaiwa and Voorhees [13]. They assume that the droplets are spherical and interacting essentially electrostatically through a concentration field with both monopole and dipole contributions. Both the droplet size distribution function and the structure factor can be extracted by numerical simulation of the equations produced by the theory. Our structure factors and those of [13] are compared in Fig. 11. Both results agree and give Porod's law at large Q. At small Q both results exhibit Q^4 behavior, although our results seem to have a smaller coefficient of Q^4 than theirs. This may also be why the widths of our peaks are consistently smaller than those of [13]. There is also significant disagreement on

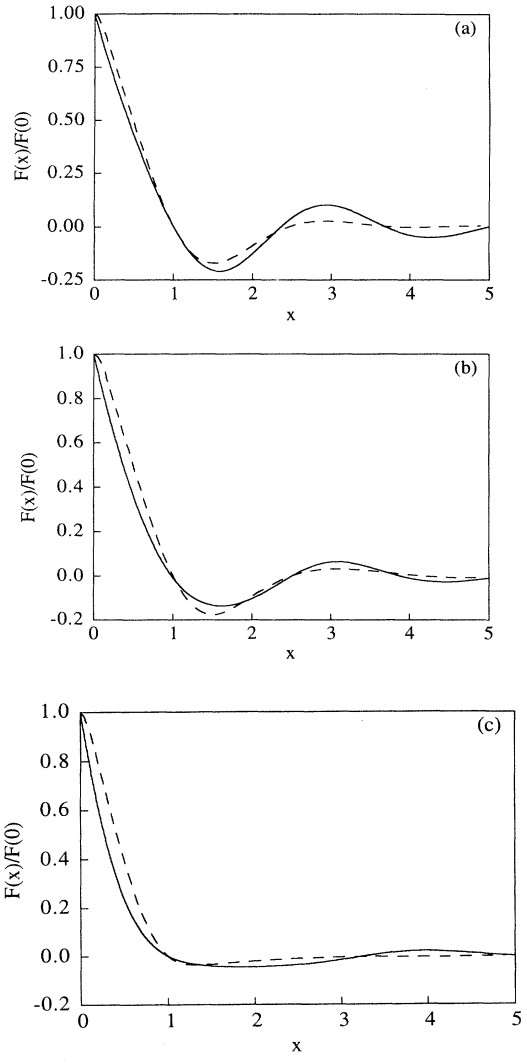

FIG. 10. A comparison of our scaling forms for the correlation function (solid lines) in two dimensions with those of [15] (dashed lines). The horizontal axis has been chosen so that the first zero of $F(x)$ occurs at $x=1$ for both functions. (a) $\phi=0.5$. (b) $\phi=0.21$. (c) $\phi=0.05$.

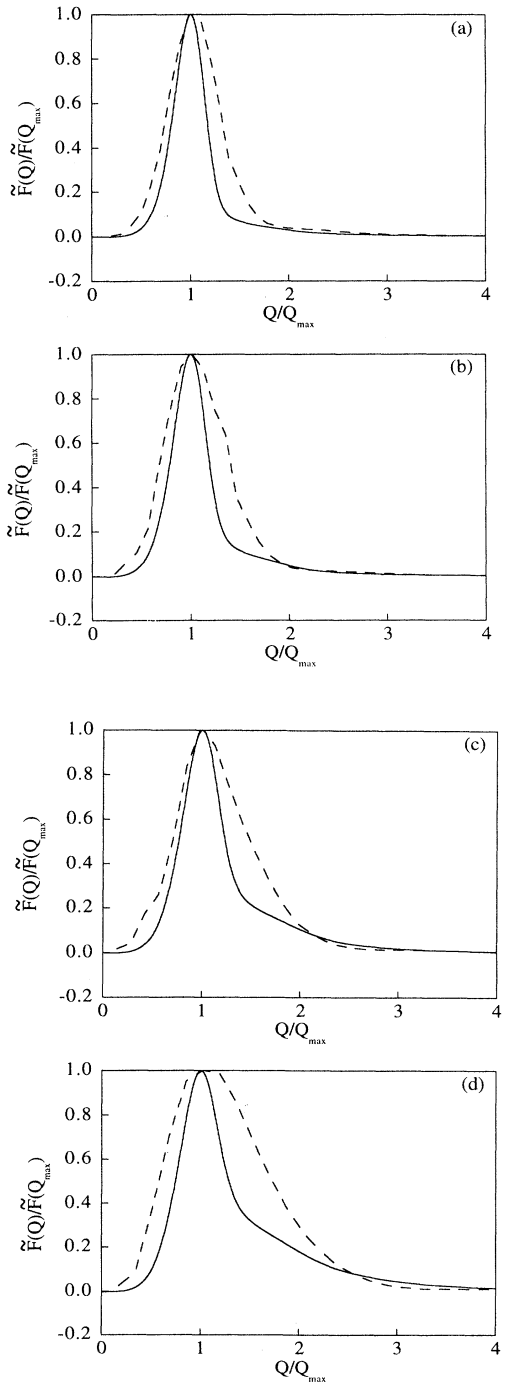

FIG. 11. A comparison of our structure factors (solid lines) in three dimensions with those of [13] (dashed lines). (a) $\phi=0.3$. (b) $\phi=0.2$. (c) $\phi=0.1$. (d) $\phi=0.05$.

the shape of the structure factor for values of Q just above the peak. In the theory presented here this regime of Q may be strongly affected by the breaking of the Tomita sum rule.

VII. CONCLUSION

In this paper, it has been shown that the theory developed in [1] can be extended to the case of off-critical quenches. The LSW $t^{1/3}$ law and the associated scaling behavior are determined for the entire concentration range. The scaling function is a function only of the parameters d and $\tilde{M}$, changing significantly only close to the coexistence curve where the oscillations observed in the critical case are damped out. The structure factor exhibits Porod's law for large Q and Q^4 behavior at small Q. This is the first theory capable of sensibly treating spinodal decomposition over the entire concentration range.

As discussed above, there are a number of virtues to this theory. However, there are also important limitations. First, we have not been able to make contact with the LSW theory in the $\tilde{M} \rightarrow 1$ limit. This will require extending the current theory (or some improved version) to treat the droplet distribution in the dilute limit. This is a difficult but, to us, interesting challenge. Second, it is clear that we must extend the theory developed here to include non-Gaussian corrections if we are to remedy the problem of $C_0(q,t)$ going negative for small q. Since one expects this quantity to enter the determination of the droplet distribution function in an important way, it is crucial to include non-Gaussian corrections if one is to make progress in this area. Non-Gaussian corrections have already been used to treat the critical COP case and this is discussed in [1]. Finally, it seems reasonable to assume that the primary reason that we do not obtain good quantitative agreement for $\tilde{F}(Q)$ and $F(x)$ is that we do not satisfy the Tomita sum rule. We speculate that in order to satisfy the Tomita sum rule, an improved treatment of the gradient term in the constitutive relation (2.5) is required.

ACKNOWLEDGMENTS

This work was supported by the NSF through Grant No. NSF-DMR-91-20719. The authors would like to thank Amitabha Chakrabarti, James Gunton, Norio Akaiwa, and Peter Voorhees for providing them with the data used in the comparisons. One of the authors (R.W.) acknowledges support from NSERC Canada.

[1] G. F. Mazenko, Phys. Rev. E **50**, 3485 (1994).
[2] I. M. Lifshitz and V. V. Slyosov, J. Phys. Chem. Solids **19**, 35 (1961).
[3] C. Wagner, Z. Elektrochemie **65**, 581 (1961).
[4] P. A. Rikvold and J. D. Gunton, Phys. Rev. Lett. **49**, 286 (1982).
[5] J. A. Marqusee and J. Ross, J. Chem. Phys. **80**, 536 (1984).
[6] H. Tomita, Prog. Theor. Phys. **71**, 1405 (1984).
[7] T. Ohta, Prog. Theor. Phys. **71**, 1409 (1984).
[8] M. Tokuyama and K. Kawasaki, Physica A **123**, 386 (1984); M. Tokuyama, Y. Enomoto, and K. Kawasaki, *ibid.* **143**, 183 (1987).
[9] H. Furukawa, Prog. Theor. Phys. **74**, 174 (1985).
[10] M. Marder, Phys. Rev. A **36**, 858 (1987).
[11] J. H. Yao, K. R. Elder, H. Guo, and M. Grant, Phys. Rev. B **47**, 14 110 (1993).
[12] A. Nakahara, T. Kawakatsu, and K. Kawasaki, J. Chem. Phys. **99**, 9853 (1993).
[13] N. Akaiwa and P. W. Voorhees, Phys. Rev. E **49**, 3860 (1994).
[14] T. M. Rogers and R. C. Desai, Phys. Rev. B **39**, 11 956 (1989).
[15] A. Chakrabarti, R. Toral, and J. D. Gunton, Phys. Rev. E **47**, 3025 (1993).
[16] There are, however, simulations of off-critical quenches for the three dimensional kinetic Ising model. See, for example, J. L. Lebowitz, J. Marro, and M. H. Kalos, Acta. Met. **30**, 297 (1982).
[17] G. F. Mazenko, Phys. Rev. E **49**, 3717 (1994).
[18] G. F. Mazenko, Phys. Rev. B **42**, 4487 (1990).
[19] H. Tomita, Prog. Theor. Phys. **72**, 656 (1984).
[20] G. Porod, in *Small Angle X-Ray Scattering,* edited by O. Glatter and L. Kratky (Academic, New York, 1982).
[21] C. Yeung, Phys. Rev. Lett. **61**, 1135 (1988); H. Furukawa, J. Phys. Soc. Jpn. **58**, 216 (1989); P. Fratzl, J. L. Lebowitz, O. Penrose, and J. Amar, Phys. Rev. B **44**, 4794 (1991).
[22] F. S. Bates and P. Wiltzius, J. Chem. Phys. **91**, 3258 (1989).
[23] Our results are only dependent on the fact that $V(\psi) \rightarrow \infty$ as $|\psi| \rightarrow \infty$ and the fact that there are two degenerate minima. For simplicity, we have chosen to examine a system with a symmetric potential, but the results of this paper are unchanged if one considers an asymmetric potential. If the potential has two degenerate minima at ψ_+ and ψ_- with $\psi_+ > \psi_-$, one has only to redefine $\psi_0 = \frac{1}{2}(\psi_+ - \psi_-)$ and $\tilde{M} = [M - \frac{1}{2}(\psi_+ + \psi_-)]/\psi_0$ to use the results of this paper. Note that in the symmetric case, $\psi_+ = -\psi_-$ and these definitions coincide with those given in the body of this paper.
[24] G. F. Mazenko, Physica A **204**, 437 (1994).
[25] G. F. Mazenko (unpublished).
[26] C. Yeung, Y. Oono, and A. Shinozaki, Phys. Rev. E **49**, 2096 (1994).
[27] B. D. Gaulin, S. Spooner, and Y. Morii, Phys. Rev. Lett. **59**, 668 (1987).
[28] Y. Oono and S. Puri, Phys. Rev. A **38**, 434 (1988); S. Puri and Y. Oono, *ibid.* **38**, 1542 (1988); A. Shinozaki and Y. Oono, Phys. Rev. E **48**, 2622 (1993).
[29] T. M. Rogers, K. R. Elder, and R. C. Desai, Phys. Rev. B **37**, 9638 (1988).
[30] A. Chakrabarti, R. Toral, and J. D. Gunton, Phys. Rev. B **39**, 4386 (1989); E. T. Gawlinski, J. Vinals, and J. D. Gunton, *ibid.* **39**, 7266 (1989).
[31] P. W. Voorhees, J. Stat. Phys. **38**, 231 (1985).